行政院國家科學委員會補助專題研究計畫期末報告

一個平行化耦合 DSMC-NS 模擬程式的精進與通用化及其應用之研究(三年)

Improvement and Generalization of a Parallelized Hybrid DSMC-NS Code and Its Applications (3 Years)

計畫類別：☑個別型計畫　　□整合型計畫

計畫編號：NSC-96-2628-E-009-136-MY3

執行期間：96 年 08 月 01 日至 99 年 07 月 31 日

計畫主持人：吳宗信

共同主持人： 陳彥升

計畫參與人員：洪捷粲、許哲維、蘇正勤

本成果報告包括以下應繳交之附件：

□ 赴國外出差或研習心得報告一份

□赴大陸地區出差或研習心得報告一份

□出席國際學術會議心得報告及發表之論文各一份

□國際合作研究計畫國外研究報告書一份

執行單位：國立交通大學機械工程學系

中　華　民　國　　99　年　10　月　25 日

行政院國家科學委員會專題研究計畫期末報告

一個平行化耦合 DSMC-NS 模擬程式的精進與通用化及其應用之研究

Improvement and Generalization of a Parallelized Hybrid DSMC-NS Code and Its Applications (3 Years)

計畫編號：NSC-96-2628-E-009-136-MY3
執行期限：96 年 08 月 01 日至 99 年 07 月 31 日
主持人：吳宗信　國立交通大學機械工程學系
共同主持人：陳彥升 財團法人國家實驗研究院國家太空中心
計畫參與人員：洪捷粲、許哲維、蘇正勤

中文摘要

許多重要問題的流場通常包含連續流體與稀薄氣體的區域. 對於這些問題的數值模擬無法僅考慮單一連續流體或分子動力學的方法來解決. 同時包含連續流體與分子動力學的複合法通常可用來解決這樣的問題. 在這三年的計畫裡, 我們改進先前所發展的平行化複合直接模擬蒙地卡羅-那威爾史托克法的程式. 在第二年的計畫中, 我們利用 NS solver 進行 ramjet 及 scramjet 進氣口附近化學反應氣流場模擬.同時發展及驗証一個針對非結構性網格的新型 mesh refinement 方法 virtual mesh refinement (VMR)以改善 DSMC solver 解析的準確度.在第三年的計畫中, 我們發展出一個 improved hybrid DSMC-NS scheme, 以 pressure-gradient 為基礎的 breakdown parameter 進行驗證及應用.

關鍵字: 平行化直接模擬蒙地卡羅法, 複合直接模擬蒙地卡羅-那威爾史托克法, VMR, scramjet.

Abstract

Several important flow problems often involve continuum and rarefied regions in the flow fields. Numerical simulations of these flows can not be done properly alone using either continuum or particle method. Hybrid of continuum and particle methods is often required to properly resolve the flow fields. In this 3-year project, we have proposed an improved parallelized hybrid DSMC-NS scheme. In the first year, we have converted the 3-D PDSC (Parallelized Direct Simulation Monte Carlo Code) into a general-purpose DSMC which features 2-D, 2-D axisymmetric and 3-D functionalities. In the second year, we have applied the NS equation solver to solve for chemical reacting flow field near the typical ramjet and scramjet. In addition, we have also developed and validated a new mesh refinement, named virtual mesh refinement, for unstructured grids. In the final year, the proposed improved hybrid DSMC-NS scheme is validated and applied to some realistic flow fields.

Keywords: parallelized DSMC, hybrid DSMC-NS code, virtual mesh refinement.

1. Introduction

Several technically important flow problems often involve continuum and rarefied regions in the flow fields. Examples include expanding reaction control system plumes from a space vehicle[2,3], hypersonic flows past a blunt body[4], expanding plumes from a rocket at high altitude[5], high compression ratio turbomolecular pump[6] and jet-type chemical vapor deposition[7], to name a few. Unfortunately, neither continuum nor rarefied flow solver can be used alone to accurately and efficiently solve the entire flow field. Thus, how to efficiently and accurately simulate this kind of flows represents a great challenge to the computational fluid dynamics community at large.

Prior studies in solving flow fields involving continuum and rarified regions employed the hybrid DSMC-NS schemes with various approaches of coupling the particle and continuum methods. Detailed reviews of these approaches can be found in Schwartzentruber and Boyd[8-9] and Wu, *et al.*[1] and references cited therein. In general, a hybrid DSMC-NS method applies the concept of spatial domain decomposition to distinguish the computational domain of rarefaction or thermal non-equilibrium to

be modeled by the DSMC method, and the computational domain of continuum to be solved by the CFD (NS, Euler or Stokes) solver. Success of such hybrid numerical method relies upon four important issues[1]: 1) Accurate and efficient method in determining the breakdown region; 2) Proper and efficient flow properties exchange at breakdown interface; 3) The effect of steadiness of the flow solution on designing data exchange at the interface; 4) Proper detection of coupling convergence. In the present paper, we focus on the first and fourth issues that can further improve the efficiency of the hybrid DSMC-NS algorithm.

Wu, *et al.*[1] has developed a parallelized hybrid DSMC-NS scheme with unstructured grids, in which a continuum breakdown parameter[10] (Kn_{max}= max[Kn_D, Kn_V, Kn_T]) where $Kn_Q=|\nabla Q|\times\lambda/Q$ and a thermal non-equilibrium indicator ($P_{Tne}=|(T_{tr}-T_{rot})/T_{tr}$) were used to determine the continuum and thermal equilibrium breakdown regions, respectively. A domain overlapping strategy, taking advantage of unstructured data format, with Dirichlet-Dirichlet type boundary conditions based on these two breakdown parameters is used iteratively to determine the choice of solvers in the spatial domain. These breakdown regions were simulated using the more expensive DSMC method, while other regions were simulated using the relatively cheaper NS equation solver. Normally, the size of the overlapping region is about 2-3 layers extending from the particle side towards continuum side to make sure the Maxwellian distribution can be applied accurately at solver-solver boundaries. Results showed that, not only the leading edge and shock, but also the boundary layer regions are identified as breakdown regions, in which large velocity gradient due to high-speed flows is often the dominating factor in determining Kn_{max}.

In brief summary, there are still several issues, which require further investigation. *First*, the inclusion of the boundary layer as the continuum breakdown region often caused slow convergence or even wrong solution of the coupling, which was also found by Schwartzentruber and Boyd[11]. Now question arises: is it truly continuum breakdown in the whole domain of boundary layer? *Second*, no automatic convergence mechanism of the coupling was tested, which is important in practice. Only constant number of iterations in both NS and DSMC were employed to obtain the final coupling solution. *Third*, the computational cost could be higher than the pure DSMC solution mainly due to the expensive DSMC simulations for several couplings. Any strategy of reducing the computational cost of DMSC should be highly welcome. This issue has been addressed by Schwartzentruber and Boyd[8-9] by using so-called "sub-relaxation" scheme in DSMC sampling and will not be discussed here. In this report, we intend to address the first two issues and hopefully we can improve the hybrid DSMC-NS algorithm to become a more practical tool in simulating flow field involving continuum and continuum/thermal equilibrium breakdown regions, such as hypersonic flows.

The present final report is organized as follows. Numerical methods are introduced briefly in Section 2, in which the NS equation solver and DSMC code are included. Section 3 presents the results of CFD simulation, validation of a virtual mesh refinement in PDSC and improved hybrid DSMC-NS scheme. In Section 4, the conclusions of the present study are summarized along with several possible future directions of research. Finally, Section 5 presents the academic achievements resulting from this 3-yar NSC project.

2. Numerical methods

2.1 The NS equation solver

The CFD methodology is based on a multi-dimensional, finite-volume, viscous, chemically reacting, unstructured grid, and pressure-based formulation. Time-varying transport equations of continuity, species continuity, momentum, total enthalpy, turbulent kinetic energy, and turbulent kinetic energy dissipation were solved using a time-marching sub-iteration scheme and are written as:

$$\frac{\partial \rho}{\partial t}+\frac{\partial}{\partial x_j}\left(\rho u_j\right)=0 \tag{1}$$

$$\frac{\partial \rho\alpha_i}{\partial t}+\frac{\partial}{\partial x_j}\left(\rho u_j\alpha_j\right)=\frac{\partial}{\partial x_j}\left[\left(\rho D+\frac{\mu_t}{\sigma_\alpha}\right)\frac{\partial \alpha_i}{\partial x_j}\right]+\omega_i \tag{2}$$

$$\frac{\partial \rho u_i}{\partial t}+\frac{\partial}{\partial x_j}\left(\rho u_j u_i\right)=-\frac{\partial p}{\partial x_i}+\frac{\partial \tau_{ij}}{\partial x_j} \tag{3}$$

$$\frac{\partial \rho H}{\partial t}+\frac{\partial}{\partial x_j}\left(\rho u_j H\right)=\frac{\partial p}{\partial t}+Q_r+\frac{\partial}{\partial x_j}\left(\left(\frac{K}{C_p}+\frac{\mu_t}{\sigma_H}\right)\nabla H\right)+\frac{\partial}{\partial x_j}\left(\left(\left(\mu+\mu_t\right)-\left(\frac{K}{C_p}+\frac{\mu_t}{\sigma_H}\right)\right)\nabla\left(V^2/2\right)\right)+\theta \tag{4}$$

$$\frac{\partial \rho k}{\partial t}+\frac{\partial}{\partial x_j}\left(\rho u_j k\right)=\frac{\partial}{\partial x_j}\left[\left(\mu+\frac{\mu_t}{\sigma_k}\right)\frac{\partial k}{\partial x_j}\right]+\rho\left(\Pi-\varepsilon\right) \tag{5}$$

$$\frac{\partial \rho \varepsilon}{\partial t}+\frac{\partial}{\partial x_j}\left(\rho u_j \varepsilon\right)=\frac{\partial}{\partial x_j}\left[\left(\mu+\frac{\mu_t}{\sigma_\varepsilon}\right)\frac{\partial \varepsilon}{\partial x_j}\right]+\rho\frac{\varepsilon}{k}\left(C_1\Pi-C_2\varepsilon+C_3\Pi^2/\varepsilon\right) \tag{6}$$

A predictor plus corrector solution algorithm was employed to provide coupling of the governing equations. A second-order central-difference scheme was employed to discretize the diffusion fluxes and source terms. For the convective terms, a second-order upwind total variation diminishing difference scheme was used. To enhance the temporal accuracy, a second-order backward difference scheme was employed to discretize the temporal terms. Details of the numerical algorithm can be found in Ref's [12)-18)].

An extended k-ε turbulence model[19] was used to describe the turbulence. A modified wall function approach was employed to provide wall boundary layer solutions that are less sensitive to the near-wall grid spacing. Consequently, the model has combined the advantages of both the integrated-to-the-wall approach and the conventional law-of-the-wall approach by incorporating a complete velocity profile and a universal temperature profile[17]. A finite-rate chemistry chemical reaction mechanism[14)-20)] was used to describe the combustion process occurs inside

the scramjet combustion chamber.

In the present numerical investigation, hydrogen/air combustion conditions are of interest. A reduced 9-step hydrogen/oxygen reaction chemical kinetics mechanism [12)-13)] is employed for the combustion simulation. This chemistry model is summarized in Table 1.

2.2 DSMC method

The direct simulation Monte Carlo (DSMC) method is a computational tool for simulating flows in which effects at the molecular scale become significant [1]. The Boltzmann equation, which is appropriate for modelling these rarefied flows, is extremely difficult to solve numerically due to its high dimensionality and the complexity of the collision term. DSMC provides a particle based alternative for obtaining realistic numerical solutions.

In this report, a new mesh-refining process (virtual mesh refinement) for DSMC using unstructured grids, which is based on the TAS (transient adaptive sub-cell) concept, is introduced to virtually refine the background cells. Virtual mesh refinement (VMR) based on the data obtained on the initial DSMC simulation using the background grid. The results of the initial DSMC simulation are used to determine the local mean free path in each background cell, which is then compared with the corresponding cell size. The result of comparison is then used to calculate the number of refined cells in each coordinate direction required to resolve the local mean free path in background cell. Note the refined cell is organized as Cartesian structured grids with the same cell size. Refined cell size is normally taken to be less than one half of the local mean free path, although it can be controlled by the user. A typical example is schematically shown in Fig. 1. One important advantage is the particle tracing becomes very efficient which results directly from the use of Cartesian structured grids for the refined cells. The sub-cell in each background cell, which contains the background cell centroid is also identified in this step. This will be used in the final data output.

In addition, area of each sub-cell ("area" in two-dimensional case; "volume" in three-dimensional case), which is geometrically inside the background cell, is calculated using the Monte Carlo (MC) method. Note the area of the sub-cell (or volume) is required in calculating the number of collision pairs such as NTC method[21)]. The reason not to apply the conventional method such as coordinate geometry is that it becomes very cumbersome and complicated as it is extended to three-dimensional case. The MC method is easy in concept as well as practical implementation, as shown schematically in Fig. 2**.** Each particle with randomly assigned position is checked if it is located in the background cell. Once it is located in the background cell, then the sub-cell which contains the particle is easily determined by taking advantage of the Cartesian structured sub-cells. Only those particles located inside the sub-cell and background cell are counted for the area calculation. The area of the *i*th sub-cell inside the background cell is thus calculated as follows:

$$V_{vc_i} = V_c \times R_i / \sum_{i=1}^{N_{vc}} R_i$$

where *Ri* is the number of particles located inside the *ith* sub-cell, *Vc* is the area of background cell and *Nvc* is the total number of sub-cells. Our experience shows that approximately 5,000**Nvc* particles are required to reach 0.1% error for area calculations of all the sub-cells, which takes about 12.5 minutes of computational time for ~300,000 virtual sub-cells using 12 processors. This computational overhead is comparatively low as compared to the total DSMC simulation in general.

2.3 Hybrid DSMC-NS method

2.3.1 Kinetic Velocity Sampling

To probe whether the boundary layer is a thermal non-equilibrium region, a direct kinetic sampling study for a supersonic wedge flow case is conducted, as schematically shown in Fig. 3. This test problem may represent an idealistic flow for studying the continuum and thermal breakdown parameter since it includes a leading edge near the tip of the wedge surface, an oblique shock wave originating from the leading edge, a boundary layer along the wedge surface, an expanding fan starting at the end of wedge surface and a highly rarefied wake behind the wedge. Sampling locations and distribution of continuum breakdown parameter Kn_{max} based on flow density, temperatures and velocities, resulting from a pure DSMC simulation, are indicated in Fig. 3.

Important flow conditions are briefly summarized as: nitrogen gas, Mach number of 4 (1,111m/s), free-stream temperature of 185.6K and wedge wall-temperature of 293.3K. DSMC related simulation conditions are the same as those described earlier[1)]. Note the Knudsen number based on the length of the wedge and the free-stream conditions is 0.0017. In addition, the thermal non-equilibrium indicator is further generalized in the present study as follows:

$$P_{Tne}^{*} = \sqrt{\frac{(\frac{T_x}{T_{tot}}-1)^2 + (\frac{T_y}{T_{tot}}-1)^2 + (\frac{T_z}{T_{tot}}-1)^2 + \zeta_{rot}(\frac{T_{rot}}{T_{tot}}-1)^2 + \zeta_v(\frac{T_v}{T_{tot}}-1)^2}{(3+\zeta_{rot}+\zeta_v)}} \quad (3)$$

where T_x, T_y and T_z are translational temperature in the x-, y-, z-direction, respectively. T_{rot}, T_v and T_{tot} are rotational, vibrational and average temperature, respectively. ζ_{rot} and ζ_v are the number of degree of freedom of rotation and vibration, respectively.

Totally 52 points, including near leading edge, oblique shock, boundary layer and expanding fan, are selected in the computational domain. Velocity distributions of three Cartesian directions at each selected point are sampled for particles up to at least 0.3 million and then are compared with the corresponding local Maxwell-Boltzmann velocity distributions to calculate the degree of continuum

breakdown in these representative points. In addition, the thermal non-equilibrium indicator P^*_{Tne} is also calculated at each selected point based on the DSMC results. In general, the Kn_D and Kn_T dominate most part of the computational domain and across the oblique shock, respectively; while Kn_V dominates near the solid wall due to the high velocity gradient in the boundary layer and wake regions. Only typical results of the kinetic velocity sampling in regions in the boundary layer are described in the following in turn. Other regions such as those near the leading edge, across the oblique shock and expansion fan are skipped due to the limit of number of pages.

Figs. 4b-4d and Figs. 5b-5d show the particle random velocity distributions at Points 26-30 and Points 31-35 near the boundary layer, respectively, along with the local Maxwell-Boltzmann distribution. Note that Points 26-30, as compared to Points 31-35, are at locations closer to the leading edge, which are expected to have larger property gradients. As shown in Fig. 1 in both regions in the boundary layer, very large breakdown parameter Kn_{max} occurs due to the large velocity gradient, especially near the solid wall (Kn_{max}>0.4). Normally these two regions in the boundary layer would be considered as continuum breakdown domains based on previously proposed criterion of Kn_{max}. Astonishingly, at Points 31-35 the velocity distributions are in very good agreement with the local Maxwell-Boltzmann distribution and the temperature variation among different degrees of freedom is very small, even with very large value of Kn_{max} (all higher than 0.05 as shown in Fig. 1).

At Points 26-30 (Fig. 4) the velocity distributions are also in excellent agreement with the local Maxwell-Boltzmann distribution, although the temperature in both x- and y-direction begins to deviate from the average temperature. Even at Point 30, which is very near the solid wall, the maximum temperature deviation to the average temperature is less than 5-6% (P^*_{Tne} =0.034). In addition, at Points 31-35 (Fig. 3), which is further downstream in the boundary layer, not only the velocity distribution agrees very well with the local Maxwell-Boltzmann distribution, but also the temperature deviation among the various degrees of freedom is very small. Even at Point 35 that is very close to the solid wall, the maximum temperature deviation is less than 3% (P^*_{Tne} =0.018). We attribute the non-breakdown of continuum and thermal equilibrium among various degrees of freedom to the fact that the particles frequently collide with the isothermal solid wall and are thermalized to the wall temperature before emitting into the region near the wall.

In Fig. 3, the continuum breakdown parameter Kn_{max} in the boundary layer region is generally higher than $Kn^{Thr.}_{max}$ =0.05 as recommended by Wang and Boyd[10]. That means the boundary layer regions would be assigned as the breakdown regions. However, it can be found the random velocity distributions in the *x*-, *y*-, *z*-direction agree excellently with the Maxwell-Boltzmann distribution, respectively, in Figs. 5b-5d. Furthermore, the value of P^*_{Tne} are lower than 0.0185 for all of the Point 31-35. Thus, we can conclude that the degree of the continuum breakdown in the locations, such as Point 31-35, is overestimated based on the previously proposed criterion of Kn_{max}. The above kinetic studies indicate that it is not necessary to utilize the DSMC method in the whole boundary layer region, even the continuum breakdown parameter Kn_{max} is very large. This observation is critical in improving the efficiency of a hybrid DSMC-NS algorithm as will be presented in Section 2.3.2.

The detailed kinetic velocity sampling proves that previously defined continuum breakdown parameter $Kn_{\max}$ can generally predict the continuum breakdown well, except in the region of the boundary layer, where the thermal equilibrium generally holds well. In this region, the NS equation solver can solve flow field efficiently and accurately with proper velocity slip and temperature jump boundary conditions. Previously, we have found that inclusion of this boundary layer region as the DSMC domain may slow down the convergence of coupling[1]. Thus, an alternative continuum and thermal-equilibrium breakdown determining strategy is required to effectively "exclude" this boundary layer region to generalize the proposed hybrid DSMC-NS algorithm.

2.3.2 Improved Hybrid DSMC-NS Algorithm

In the previously proposed hybrid DSMC-NS algorithm using unstructured grids[1], steady-state flow calculation was assumed. Two breakdown parameters were used to identify the breakdown region and were defined earlier in Section 1. General procedures of iterative coupling between DSMC and NS solvers are summarized as: **1**) Simulate the whole domain using the NS solver; **2**) Determine the breakdown regions based on distribution of breakdown parameters Kn_{max} and P_{Tne} ; **3**) Extend the breakdown domain with few overlapping layers towards continuum domain; **4**) Simulate the breakdown domain using the DSMC solver; **5**) Repeat Step **1**) (but only for the continuum domain) through Step **4**) until convergence is reached.

In the present report, we use the UNIC-UNS NS solver [12-20], instead of the HYB3D as used in our previous study [1] The present Navier-Stokes equation solver, developed by Chen and his coworkers, employs the cell-centered finite-volume method with a hybrid 2D/3D unstructured-grid topology. Details of various numerical and physical modules embedded in this solver can be found in [12-20] and are skipped here for brevity. Only three important features are mentioned here. The first is the use of pressure-based method, which allows accurate simulation of the flows at all speeds. The second is the automatic slip velocity and temperature jump boundary conditions near solid wall. The third is parallel computing of the NS equation solver also incorporates the graph-partition tool, PMETIS[15], which is the same as that in the present parallelized

DSMC solver (PDSC) [21-23].

As mentioned earlier, by applying the Kn_{max} as the breakdown parameter in addition to the thermal non-equilibrium indicator P_{Tne}, the boundary layer region is generally included as the breakdown DSMC domain for high-speed flows, which generally slows down the convergence of the coupling between two numerical solvers. In the present study we define a new continuum breakdown parameter Kn_p to replace the role of Kn_{max} as follows,

$$Kn_p = \frac{\lambda}{p}|\nabla p|$$

For example, Fig. 6 shows the initial breakdown domains using the new breakdown parameter (Kn_p>0.05) based on the solution of initial NS simulation. With this new breakdown parameter, most of the boundary layer can be excluded as one of the breakdown regions, in which the more efficient NS equation solver can solve the flow field with proper slip boundary conditions at wall. However, this may induce another slow convergence of coupling, although not necessary. The reason is that, based on the initial whole-domain NS simulation, we are not able to detect the thermal non-equilibrium near the leading edge since the UNIC-UNS is a single-temperature NS equation solver like most of the others. This results in a very small breakdown region, based on the Kn_p, along the boundary layer near the leading edge. In the present study, we remove this by extending the breakdown interface 25 overlapping layers toward continuum side along the boundary layer.

In brief summary, general procedures of newly proposed hybrid algorithm are summarized as follows: **1**) Simulate the whole domain using the NS solver; **2**) Calculate breakdown parameters, Kn_p and P_{Tne} based one-shot NS simulation or the hybrid solution from NS equation and DSMC solvers; **3**) Determine the breakdown regions based on these two breakdown parameters in the whole flow field; **4**) Estimate the location of thermal breakdown interface in regions near boundary layer by extending more layers; **5**) Extend the breakdown domain with few overlapping layers towards continuum domain; **6**) Simulate the breakdown domain using the DSMC solver; **7**) Repeat Step **1**) (but only for the continuum domain) through Step **6**) until convergence is reached.

3. Results and Discussion

3.1 N-S equation solver

3.1.1 Ramjet Inlet Flow

The experimental study of an axisymmetric ramjet inlet flow was performed by Nagarathinam [25]. The half angle of the inlet spike is 20 degrees. The experimental test conditions are Mach 2.18 frees-tream, 296,000 Pa total pressure and 300 K total temperature. The strut that holds the center body to the cowl casing is omitted in the numerical computation.

To represent this model numerically, a mesh with 29,820 elements is generated (grid unit: 5 cm), which gives good grid resolution of the flow inside the inlet. The backpressure effect is provided using a porosity model, which represents the blockage effects in the flowfield downstream of the center body. A converged solution is obtained in 60,000 time steps with a 1.0E-06 sec time step size, which takes 60.6 minutes CPU time using 8 processors with 99 percent parallel efficiency. This solution takes longer to run due to the need to adjust the blockage porosity to match the backpressure of the experiment.

The predicted pressure field in the ramjet inlet is shown in Fig. 7, which indicates pressure recovery due to applied flow blockage effect downstream of the inlet that matches the test conditions. Fig. 8 illustrates the predicted Mach number distributions of the ramjet inlet. For supersonic flow computations, numerical accuracy is critical in order to keep numerical diffusion low so as not to affect the resolution of flow and shock structures.

3.1.2 Scramjet Inlet Flow

The experimental investigation of this test case was conducted by Yanta et al. [26]. The inlet geometry consists of a forebody wedge angle of 10 degrees and a 13-degree inward turning duct (inner wall turning radius of 0.057 m). The test conditions of this experiment are Mach 4 free-stream, 101,350 Pa static pressure and 311 K static temperature.

A mesh with 36,580 cells is generated for numerical computation (grid unit: 10 cm), which gives good grid resolution of the flow inside the inlet. A converged solution is obtained in 10,000 time step with a 3.0E-06 sec time step size, which takes 15.2 minutes CPU time using 8 processors with 99.2 percent parallel efficiency.

The predicted scramjet inlet pressure field is shown in Fig. 9, which gives clear resolution of the shock train system in the inlet duct. Again, for supersonic flow calculations, numerical accuracy is critical such that minimum numerical diffusion can be kept for good flow structure resolution. As a part of the present numerical tests, a first-order upwind scheme was tried, which ends up with a false bow shock upstream of the cowl lip and destroy the shock structure in the inlet duct. Fig. 10 shows the predicted temperature contours. A high temperature region is predicted along the bottom wall just downstream of the inlet turn. This is caused by cowl lip shock interaction with the bottom wall boundary layer that separates and forms a steady recirculation region where high temperature recovery occurs. This flow separation feature is also revealed in Figs. 11 and 12 of Mach number contour plots. Similar flow phenomenon is also observed in the experiment. For scramjet inlet designs, the cowl lip shock strength should be controlled by geometry tailoring such that this flow separation phenomenon can be avoided.

3.2 DSMC method

We have developed a two-level virtual mesh refinement (VMR) method and implemented in the parallelized direct simulation Monte Carlo code (PDSC) which utilizes unstructured grids. The implementation was validated by simulating one hypersonic flow and compared the results with the benchmark solution. Figure 13 shows the sketch of the Mach-15 hypersonic flow past a cylinder and related positions of presenting the profiles of properties, which is used for verification of the VMR implementation in PDSC. Important free-stream flow conditions include: argon gas, velocity of 3246 m/s, temperature of 135 K, number density of 1.41E21 m-3, Mach number of 15, and wall temperature of 300 K. Corresponding free-stream Knudsen number is 0.06 based on the free-stream mean free path ($\lambda\infty$=0.000981 m) and the diameter of the cylinder (D=0.3048 m).

Figure 14 shows the pressure distribution around the scramjet. The flow after the first oblique shock impinges on the upper leading edge, which causes reflected shock to interact with the boundary layer flow along the bottom ramp. Finally, the flow inside the horizontal channel becomes a typical channel flow and further expands to the ambient at the exit. The flow just behind the reflected shock near the upper channel wall becomes stagnant and thus high-pressure. The flow phenomena are reflected from Figure 15 and 16, which show the surface properties along the upper and lower channel wall, respectively. Results clearly show that the proposed VMR algorithm in PDSC can faithfully reproduce benchmark results with a much reduced cost up to 3-5 times.

3.3. Improved Hybrid DSMC-NS Method

3.3.1 Test problem

3.3.1 Flow and Simulation Conditions

Similar to previous study[1)], a supersonic nitrogen flow (M_∞=4) past a 2-D wedge of 25° half-angle with a length of 60.69 mm is chosen as the test problem for the new hybrid algorithm. All simulation conditions are the same as those in previous study and summarized in Table 2. In this study, number of extension layers is fixed as four, except near the boundary layer close to the leading edge. Some of the simulation conditions are mentioned in the following, as it is necessary. In addition, 10 processors are used throughout the study.

3.3.2 Distribution of Breakdown Domains

The final distribution of breakdown domains using Kn_p and P_{Tne} after 20 coupling iterations is illustrated in Fig. 17. Note the criterion for Kn_p and P_{Tne} is set as 0.05 and 0.03, respectively, in this study, unless otherwise specified. Note the breakdown domain only includes the regions across the shock and regions near the leading edge, in which most boundary layer regions are excluded, which the NS equation solver can be used to obtain the flow field more efficiently, while accurately enough.

3.3.3 Comparison of the New Hybrid DSMC-NS Algorithm with the Pure DSMC Method

Fig. 18a and Fig. 18b compare the contour distributions of density and translational temperature both obtained from the pure DSMC simulation and the improved hybrid DSMC-NS algorithm, respectively. The results of the present coupled algorithm are in excellent agreement with those of pure DSMC simulation. Detailed comparisons of density, velocity magnitude and temperature profiles obtained from the present coupled algorithm, pure DSMC and pure NS equation solvers are also very favorable, but they are not presented in the present paper due to the limit of the paper length.

3.3.4 Comparison of Convergence between the Old and New Coupled Algorithms

Table 2 summarizes the simulation conditions along with the breakdown criteria for the old and new coupled algorithm for this specific test case. Results show that fewer DSMC cells are included in the new algorithm as compared to that in the old one. This reduction of number of DSMC cells and fewer coupled iterations required attributes to the shorter simulation time as summarized in Table 3. New algorithm can save up to 50% of the computational cost with the same convergence criteria for the present test case. Note this problem is chosen such that the pure DSMC solution can be obtained in a short period of time.

As mentioned earlier, varying the size of the overlapping regions and the criteria of breakdown parameters may have an impact on the convergence rate, computational cost and accuracy of solutions. Figs. 19a and 19b illustrate the convergence history of L2-norm deviation of density and overall temperature, respectively, with different breakdown criteria. Result shows the L2-norm deviations of the new hybrid algorithm level off starting at the 6th iteration, while they take up to 10 iterations with obviously higher values for the old hybrid algorithm. The adoption of the new breakdown criteria indeed improves the efficiency of coupling convergence. As compared to the results after 20 iterations, it only takes 4 coupling iterations with new breakdown criterion Kn_p for reaching a well converged solution, while it needs at least 6 or 7 using the old Kn_{max}.

3.4 Application Case

3.4.1 Flow and Simulation Conditions

Hypersonic nitrogen flow past a 2-D square cylinder shown in Fig. 20 is chosen as the application case for the coupled algorithm. Free-stream conditions for this test case include: gaseous nitrogen as the flowing fluid, a Mach number (M_∞) of 12, a velocity (U_∞) of 1,547 m/s, a density (ρ_∞) of 9.54E-5 kg/m^3 and a temperature (T_∞) of 40 K and the solid wall boundary is adiabatic. Note the threshold values for Kn_p and P_{Tne} are set as 0.05 and 0.1, respectively.

Related simulation conditions are also summarized in Table 4 for reference.

3.4.2 Distribution of Breakdown Domains

Fig. 20 shows the final breakdown regions after 20 coupling iterations based on the simulation condition. Lines A-E are selected to compare the results among pure DSMC, pure NS equation solver (NSS), 3 and 20 hybrid DSMC-NS iterations. Note the breakdown domain only includes the regions across the shock, and zones near the leading edge and wake region. We can see most boundary layer regions are excluded, which the NS equation solver can be used to obtain the flow field more efficiently. Fig. 21 illustrates the profiles of continuum breakdown parameter Kn_p along Line B. The horizontal dashed line showing the threshold value Kn_P at which the continuum breaks down and the NS equation solver cannot be used.

General trend of the Kn_P distribution shows that the value is rather large (up to 0.4 or larger) near the shoulder of square cylinder due to large property gradients in leading edge region, and decreases to rather small value in the region between the boundary layer and the oblique shock, and finally becomes large again across the oblique shock (up to 0.5 or less). Obviously, the Kn_P distribution from either 3 or 20 coupled DSMC-NS iteration is in good agreement with those by pure DSMC simulation while pure NS equation solver predicts a much thinner shock length and different location of oblique shock.

Fig. 21a and Fig. 21b show contour distributions of density and translational temperature from the pure DSMC simulation and the coupled DSMC-NS algorithm, respectively. Results of the present coupled algorithm are in good agreement with those of pure DSMC simulation. Fig. 23 illustrates detail comparisons of density, translational temperature and profiles along Line B while the other lines are not presented in the present paper due to the limitation of paper length. Based on the calculated breakdown parameters (Kn_P and P_{Tne}), the flow region is divided into four sub-domains, as shown in Fig. 23a: Zone I and Zone III are the DSMC solution domains, while the other two regions (II and VI) are the NS solution domains. At this location (along Line B), the results of the NS equation solver deviate appreciably from those of both pure DSMC simulation and the coupled method (after either 3 or 20 iterations). Results of the present hybrid methods are still in excellent agreement with those of pure DSMC simulation for the entire domain. It also shows 3 hybrid iterations are good enough to reach convergence of the hybrid algorithm. Related computational timings are listed in Table 5 for reference.

4. Conclusion

In this 3-year NSC project, we have: 1) applied the NS equation solver to simulate reacting flow field near the ramjet and scramjets; 2) developed and validated a VMR algorithm in PDSC and 3) developed and demonstrated an improved DSMC-NS scheme. The first one shows that the present NS equation solver can predict important features of these challenging supersonic to hypersonic flows. The second show that the newly proposed VMR can faithfully reproduce the benchmark solution with a much reduced computational cost. An improved parallel hybrid DSMC-NS algorithm is proposed and verified in the project. Direct kinetic velocity sampling is conducted to point out that previously defined continuum breakdown parameter $Kn_{\max}$ could overestimate the degree of the continuum breakdown in most region of the boundary layer, where the thermal equilibrium generally holds well. A new breakdown Kn_P based on pressure is designed to effectively "exclude" such that boundary layer region. A 2-D 25-degree wedge flow (M_∞=4) was used as the test case for verification of the improved hybrid method. Most of the boundary layer region can be excluded as the breakdown region, if the breakdown parameter Kn_p is employed. With this new hybrid algorithm, simulation converges faster as compared to the old one. Then, this improved algorithm is applied to a hypersonic flow (M_∞=12) pass a square cylinder case. Results show that, with the proposed coupled algorithm, simulation can obtain a good solution within 3 coupling iterations.

5. Self-Evaluation

在本計畫資助之下，本人已成功在交通大學建立一個具國際水準的大型模擬研究團隊，同時研究成果亦相當豐碩。**總計在過去三年中(2007-2010)在hybrid DSMC-NS 及kinetic-based scheme方面已經發表6篇的SCI期刊論文 [1-6], 2篇審查中的SCI期刊論文[7-8]及33篇國際會議論文及[9-41]。**

Publication List: 2007-2010 (J.-S. Wu)

1. H.M. Cave, K.-C. Tseng, **J.-S. Wu***, M.C. Jermy, J.-C. Huang and S.P. Krumdieck, "Implementation of Unsteady Sampling Procedures for the Parallel Direct Simulation Monte Carlo Method," Journal of Computational Physics, Vol. 227, pp. 6249-6271, 2008.
2. M.R. Smith, H.M. Cave, **J.-S. Wu***, Y.-S. Chen and M.C. Jermy, "An Improved Quiet Direct Simulation Method for Eulerian Fluids Using a Second-Order Scheme," Journal of Computational Physics, Vol. 228, pp. 2213-2224, 2009.
3. C.-C. Su, K.C. Tseng, H.M. Cave, Y.Y. Lian, T.C. Kuo, M.C. Jermy, and **J.-S. Wu***, "Implementation of a Transient Adaptive Sub-Cell Module for the Parallel DSMC Code Using Unstructured Grids," Computers & Fluids, Vol. 39, pp. 1136-1145, 2010.
4. Matthew R. Smith, Fang-An Kuo, David Hsieh, Jen-Perng Yu, **J.-S. Wu*** and Alex Ferguson, "Rapid Optimization of Blast Wave Mitigation Strategies using Quiet Direct Simulation and Genetic Algorithm," Computer Physics Communications, Vol. 181, pp. 1025-1036, 2010.
5. A. Ferguson, M.R. Smith and **J.-S. Wu***, "Accurate True Direction Solutions to the Euler Equations Using a Uniform Distribution Equilibrium Method," Computer Modeling in Engineering and Science (**proofread** on September 1, 2010).
6. Matthew R. Smith*, Fang-An Kuo, Chih-Wei Hsieh, Chau-Yi Chou and **Jong-Shinn Wu***, "Hybrid Parallelization of a

Rapid True Direction Kinetic Flux Scheme using MPI and GPU Computation," Computers & Fluids (**accepted**, 2010)

7. C.-C. Su, K.-C. Tseng, **J.-S. Wu*** H.M. Cave, M.C. Jermy and Y.-Y. Lian, "Two-level Virtual Mesh Refinement Algorithm in a Parallelized DSMC Code Using Unstructured Grids," Computers & Fluids (submitted on April 27, 2010)
8. Yu-Yung Lian, Yen-Sen Chen, K.-C. Tseng, **Jong-Shinn Wu***, Bill Wu and Luke Yang, "Improved Parallelized Hybrid DSMC-NS Scheme," Computers & Fluids (submitted on September 1, 2010).
9. **J.-S. Wu***, K.-C. Tseng, Y.-Y. Lian, H.M. Cave, J.-P. Yu, Y.-S. Chen, "Recent Progress in Developing a General-purpose Parallelized Direct Simulation Monte Carlo Code (PDSC) Using Unstructured Grid," The 4th Japan-Taiwan Workshop on Mechanical and Aerospace Engineering, Hakone Prince Hotel, Kanagawa, Japan, October 29-30, 2007. (**invited speech**)
10. K.-C. Tseng, T.-C. Kuo, Y.-J. Lin, C.-C. Su, **J.-S. Wu**, "Parallel Computing of DSMC and Its Applications In Rarefied Gas Regime," Workshop on High Performance Simulation of Physical Systems, HPSPS' 09, March 2-5 (2009), Kaohsiung, Taiwan. (**invited speech**)
11. Hadley Cave, Matthew Smith, Mark Jermy, **J. S. Wu***, "Gas dynamics simulations using the Quiet Direct Simulation method," Workshop on High Performance Simulation of Physical Systems, HPSPS' 09, March 2-5 (2009), Kaohsiung, Taiwan. (**invited speech**)
12. Kun-Chang Tseng, T.-C. Kuo, Cheng-Chin Su, Ya-Ju Lin, **J.-S. Wu***, "Parallel Computing of DSMC and Its Applications in Rarefied Gas Regime," Workshop on High Performance Simulation of Physical Systems, HPSPS' 09, March 2-5 (2009), Kaohsiung, Taiwan. (**invited speech**)
13. M.R. Smith, H.M. Cave, Y.-J. Lin, F.-A. Kuo, **J.-S. Wu***, M.C. Jermy, C.-W. Lim and Y.-S. Chen, "Overview and outlook of the quiet direct simulation method as a flow solver," The Fifth Taiwan -Japan-Workshop on Mechanical and Aerospace Engineering, Chi-Tou, Nantou, Taiwan, Oct. 21-24, 2009.
14. Matthew Smith*, Fang-An Kuo, Chih-Wei Hsieh, Chau-Yi Chou, **Jong-Shinn Wu**, "Hybrid of a Rapid True Flux Scheme using MPI and GPU," The 22nd International Conference on Parallel Computational Fluid Dynamics, Kaohsiung, Taiwan, May 17-21, 2010. (Invited Speech)
15. H.M. Cave, J.-C. Huang, **J.-S. Wu**, S.P. Krumdieck, K.-C. Tseng, M.C. Jermy, M. Lebedev, K.-W. Cheng and Y.-S. Chen, "Flow Field Modelling of Pulsed Pressure Chemical Vapour Deposition," Sixteenth European Conference on Chemical Vapor Deposition September 16-21, 2007, Den Haag (Scheveningen), The Netherlands.
16. **J.-S. Wu*,** K.-C. Tseng, H.M. Cave, Y.-Y. Lian, J.-P. Yu, Y.-S. Chen, M.C. Jermy and S.P. Krumdieck, "Developing a General-Purpose Parallelized Direct Simulation Monte Carlo Code (PDSC) Using Unstructured Grid: A Progress Report," DSMC: Theory, Methods and Applications, Santa Fe, New Mexico, USA, September 30-October 3, 2007.
17. Y.-Y. Lian, **J.-S. Wu***, K.-C. Tseng, Y.-S. Chen, "Development of an Improved Parallelized Hybrid DSMC-NS Algorithm and Its Applications in Hypersonic Flow Computation", 26th International Symposium on Space Technology and Science (ISTS), June 1-8, 2008, Hamamatsu City, Japan.
18. Y-Y. Lian, K-C. Tseng, Y.-S. Chen, M.-Z. Wu, J.-S. Wu* and Gary Cheng, "An Improved Parallelized Hybrid DSMC-NS Algorithm and Its Applications in Hypersonic Flows," 26th International Symposium on Rarefied Gas Dynamics, July 21-25, 2008, Kyoto University,Kyoto,Japan.
19. H.M. Cave, M.C. Jermy, K.C. Tseng and J.S. Wu, "DREAM: An Efficient Methodology for DSMC Simulation of Unsteady Processes," 26th International Symposium on Rarefied Gas Dynamics, July 21-25, 2008, Kyoto University,Kyoto,Japan.
20. K.C. Tseng, H.M. Cave, T.C. Kuo, M.C. Jermy, S.P. Krumdieck and **J.-S. Wu***, "Implementation of the Transient Adaptive Sub-Cell Module for the Parallel DSMC Code," 26th International Symposium on Rarefied Gas Dynamics, July 21-25, 2008, Kyoto University,Kyoto,Japan.
21. C.-C. Su, **J.-S. Wu***, K.-C. Tseng, J.-P. Yu and Y.-Y. Lian, "Two-level Virtual Mesh Refinement Algorithm in a Parallelized DSMC Code Using Unstructured Grids," 26th International Symposium on Rarefied Gas Dynamics, July 21-25, 2008, Kyoto University,Kyoto,Japan.
22. Hadley M. Cave, Chin-Wai Lim, Mark C. Jermy, **Jong-Shinn Wu***, Matthew R. Smith and Susan P. Krumdieck, "CVD flow field modelling using the Quiet Direct Simulation (QDS) method," The 17th European CVD Conference, 2009.
23. Hadley M. Cave, Matthew R. Smith,, Mark C. Jermy, **J.-S. Wu***, "Gas dynamics simulations using the QDS method," HPC-Asia 2009, March 2-5 (2009), Kaohsiung, Taiwan. **(Invited speaker)**.
24. **M.R. Smith***, F.-A. Kou, C.-Y. Chou and J.-S. Wu, "Application of a kinetic theory based solver of the Euler equations using GPU," The 21st International Conference on Parallel CFD, May 18-22, 2009, Moffett Field, California, USA.
25. C.-C. Su, K.-C. Tseng, **J.-S. Wu***, J.-P. Yu and Y.-Y. Lian, "Development of a Virtual Mesh Refinement Algorithm in a Parallel Unstructured-grid DSMC Code," The 21st International Conference on Parallel CFD, May 18-22 (2009), Moffett Field, California, USA.
26. C.W. Lim, Z. Zaino Abidin, H.M. Cave, M.C. Jermy, **J.-S. Wu***, M.R. Smith and S.P. Krumdieck, "Numerical simulations of unsteady inviscid flow using the quiet direct simulation method," PSFVIP-7: The 7th Pacific Symposium on Flow Visualization and Image Processing, Kaohsiung, Taiwan, Nov 16th-19th, 2009.
27. C.C. S, K.C. Tseng, H.M. Cave, **J.-S. Wu***, Y.Y. Lian, T.C. Kuo and M.C. Jermy, "Development of a transient adaptive sub-cell (TAS) module for the unstructured-grid direct simulation Monte Carlo (DSMC) method," PSFVIP-7: The 7th Pacific Symposium on Flow Visualization and Image Processing, Kaohsiung, Taiwan, Nov 16th-19th, 2009.
28. Cheng-Chin Su, Matthew Smith, David Hsieh, and **J.-S. Wu***, "Two-Dimensional Direct Simulation Monte Carlo Computation Using GPUs," Conference on Computational Physics (CCP) 2009, Kaohsiung, Taiwan, December 15-19, 2009.
29. Y.-J. Lin, M. Smith, Fang-An Kuo, H. Cave, **J.-S. Wu***, "Two-dimensional quiet direct simulation (QDS) using GPUs," Conference on Computational Physics (CCP) 2009, Kaohsiung, Taiwan, December 15-19, 2009.
30. H.M. Cave, M.R. Smith, Y.-J. Lin, F.-A. Kuo, **J.-S. Wu***, M.C. Jermy, and C.-W. Lim, "Overview of the Kinetic-based Quiet Direct Simulation (QDS) Method for Gas Flow Computation," The 8th Asian Computational Fluid Dynamics Conference, Hong Kong, 10-14 January 2010.
31. Matthew Smith*, Fang-An Kuo, Chih-Wei Hsieh, Chau-Yi Chou, **Jong-Shinn Wu**, "Hybrid of a Rapid True Flux Scheme using MPI and GPU," The 22nd International Conference on Parallel Computational Fluid Dynamics, Kaohsiung, Taiwan, May 17-21, 2010. (Invited Speech)
32. H.M. Cave, M .R. Smith, J.-S . Wu, M .C. J ermy, Y.-J. L in, C.- W. Lim , S.P. K rumdieck, "Multispecies Fluxes for the Parallel Quiet Direct (QDS) Method," The 22nd International Conference on Parallel Computational Fluid Dynamics, Kaohsiung, Taiwan, May 17-21, 2010.
33. C.-C. Su, Chih-Wei Hsieh, Smith, **J.-S. Wu***, Kun-Chang Tseng, "Parallel DSMC Computation Using GPUs," The 22nd International Conference on Parallel Computational Fluid Dynamics, Kaohsiung, Taiwan, May 17-21, 2010.
34. Chin Wai Lim, Hadley Cave, Mark Jermy*, **Jong-Shinn Wu**, Susan Krumdieck, "Numerical Simulation of Low Pressure Flows in Pulsed Pressure Chemical Vapor Deposition Process

using the Quiet Direct Simulation, The 22nd International Conference on Parallel Computational Fluid Dynamics, Kaohsiung, Taiwan, May 17-21, 2010.

35. Kun-Chang Tseng*, Tien-Chuan Kuo, **Jong-Shinn Wu**, "Validation and Sensitivity Studies of the Cold Gas Propulsion System by Using the DSMC Method," The 22nd International Conference on Parallel Computational Fluid Dynamics, Kaohsiung, Taiwan, May 17-21, 2010.
36. Yu-Yung Lian*, Yen-Sen Chen, K.-C. Tseng, **Jong-Shinn Wu**, Bill Wu, Luke Yang, "Concurrent Parallelized Hybrid DSMC-NS Method," The 22nd International Conference on Parallel Computational Fluid Dynamics, Kaohsiung, Taiwan, May 17-21, 2010.
37. H.M. Cave, C.-W. Lim, M.C. Jermy*, S.P. Krumdieck, M.R. Smith, Y.J. Lin and **J.-S. Wu**, "Multi-Species Fluxes for the Parallel Quiet Direct Simulation (QDS) Method," The 27th International Symposium on Rarefied Gas Dynamics, California, July 10-16, 2010.
38. Y.-J. Lin, M. R. Smith, H. M. Cave, J.-C. Huang and **J.-S. Wu***, "General Higher Order Extension to the Quiet Direct Simulation Method," The 27th International Symposium on Rarefied Gas Dynamics, California, July 10-16, 2010.
39. C.-C. Su, **J.-S. Wu***, C.-W. Hsieh and M.R. Smith, "Parallel Direct Simulation Monte Carlo Computation Using CUDA on GPUs," The 27th International Symposium on Rarefied Gas Dynamics, California, July 10-16, 2010.
40. C.W. Lim, H.M. Cave, M.C. Jermy*, S.P. Krumdieck and **J.-S. Wu**, "An Approximate Method for Solving Unsteady Transitional and Rarefied Flow Regimes in Pulsed Pressure Chemical Vapour Deposition Process using the Quiet Direct Simulation Method," The 27th International Symposium on Rarefied Gas Dynamics, California, July 10-16, 2010.
41. M.R. Smith*, F.-A. Kuo, H.M. Cave, M.C. Jermy and **J.-S. Wu**, "Quiet Direct Simulation (QDS) of Viscous Flow Using the Chapman-Enskog Distribution," The 27th International Symposium on Rarefied Gas Dynamics, California, July 10-16, 2010.

References

1. Wu, J.-S., Lian, Y.-Y., Cheng, G., Koomullil, R. P. and Tseng, K.-C.: Development and Verification of a Coupled DSMC-NS Scheme Using Unstructured Mesh, *J. Comput. Phys*, **219** (2006), pp. 579-607.
2. Taniguchi, M., Mori, H., Nishihira, R. and Niimi, T.: Experimental analyses of flow field structures around clustered linear aerospike nozzles, *AIP Conference Proc.*, **762** (2005), pp. 349-354.
3. Ivanov, M. S., Khotyanovsky, D. V., Kudryavtsev, A. N., Vashchenkov, P. V., Markelov, G. N., Schmidt, A. A.: Numerical study of backflow for nozzle plumes expanding into vacuum, *AIAA Paper 2004-2687* (2004).
4. Moss, J. N., Price, J. M.: Survey of Blunt Body Flows including wakes at Hypersonic Low-Density Conditions, J. Thermophysics & Heat Transfer, Vol. 11, No. 3, pp. 321-329, 1997.
5. Wilmoth, Richard G., Yellin, Keith A. and Papp, John L.: Continuum-DSMC Coupling Issues for Steady and Unsteady Two-Phase Plumes, *28th EPTS and 10th SPIRITS User Group Joint Meeting*, San Diego, 2004.
6. Cheng, H.-P., Jou, R.-Y., Chen, F.-Z., and Chang, Y.-W.: Three-Dimensional Flow Analysis of Spiral-Grooved Turbo Booster Pump in Slip and Continuum Flow, *J. Vacu. Sci. Tech. A: Vacuum, Surface, and Films*, **18** (1999), pp. 543-551.
7. Versteeg, V., Avedisian, C. T. and Raj, R.: Method and Apparatus for CVD Using Liquid Delivery System with an Ultrasonic Nozzle, *U.S Patent Number: 5,451,260* (1994).
8. Schwartzentruber, T. E., Boyd, I. D.: A hybrid particle-continuum method applied to shock waves, *J. Comput. Phys.*, **215** (2006), pp.402-416.
9. Schwartzentruber, T. E., Scalabrin, L. C. and Boyd, I. D.: A modular particle-continuum numerical method for hypersonic non-equilibrium gas flows, *J. Comput. Phys.*, **225** (2007), pp. 1159-1174.
10. Wang, W.-L. and Boyd, I. D.: Predicting Continuum Breakdown in Hypersonic Viscous Flows, *Physics of Fluids*, **15** (2003), pp. 91-100.
11. Schwartzentruber, T. E., Scalabrin, L. C. and Boyd, I. D.: Progress on a Modular Particle-Continuum Numerical Method for Multi-Scale Hypersonic Flows, *DSMC Theory, Methods, and Applications Conference*, NM., 2007.
12. Wang, T.S., Chen, Y.S., "Unified Navier-Stokes Flowfield and Performance Analysis of Liquid Rocket Engines," *J. Propulsion and Power*, Vol. 9, No. 5, pp. 678-685, 1993.
13. Chen, Y.-S., Liu, J., Zhang, S., and Mallapragada, P., "An Integrated Tool for Launch Vehicle Base-Heating Analysis," Final Report, NAS8-00002, Engineering Sciences, Inc., Huntsville, AL, 2001.
14. Liaw, P., Shang, H.M., Chen, Y.S., "Particulate Multi-Phase Flowfield Calculation with Combustion/Breakup Models for Solid Rocket Motor," AIAA-94-2780, 30th AIAA/ASME/SAE/ASEE Joint Propulsion Conference, June 27-29, 1994, Indianapolis, IN.
15. Chen. Y.-S., Zhang S., and Liu, J., "Stage Separation Performance Analysis Project," Final Report, H-34345D, Engineering Sciences, Inc., Huntsville, AL, 2002.
16. Wang, T.-S., Chen, Y.-S., Liu, J., Myrabo, L.N., and Mead, F.B. Jr., "Advanced Performance Modeling of Experimental Laser Lightcraft," *Journal of Propulsion and Power*, Vol. 18, No. 6, 2002, pp. 1129-1138.
17. Wang, T.-S., "Multidimensional Unstructured-Grid Liquid Rocket Engine Nozzle Performance and Heat Transfer Analysis," *Journal of Propulsion and Power*, Vol. 22, No. 1, 2005, pp. 78-84.
18. Wang, T.-S., "Transient 3-D Analysis of Nozzle Side Load in Regeneratively Cooled Engines," AIAA Paper 2005-3942, 41st AIAA/ASME/SAE/ASEE Joint Propulsion Conference, Tucson, Arizona, 2005.

19. Chen, Y.-S., and Kim, S. W., "Computation of Turbulent Flows Using an Extended k-ε Turbulence Closure Model," NASA CR-179204, 1987.
20. Wang, T.-S., "Thermophysics Characterization of Kerosene Combustion," *Journal of Thermophysics and Heat Transfer*, Vol. 15, No. 2, 2001, pp.140-147.
21. Wu, J.-S. and Tseng, K.-C.: Parallel DSMC Method Using Dynamic Domain Decomposition, *International Journal for Numerical Methods in Engineering*, **63** (2005), pp. 37-76.
22. Wu, J.-S., Tseng, K.-C. and Wu, F.-Y.: Parallel Three Dimensional Direct Simulation Monte Carlo Method Using Unstructured Adaptive Mesh and Variable Time Step, *Computer Physics Communications*, **162** (2004), pp. 166-187.
23. Wu, J.-S. and Tseng, K.-C., Lee, U.-M. and Lian, Y.-Y.: Development of a General Parallel Three-Dimensional Direct Simulation Monte Carlo Code, *AIP Conference Proceedings*, **762** (2005), pp. 559-564.
24. G.A. Bird, *Molecular Gas Dynamics and the Direct Simulation of Gas Flows*, Oxford University Press, 1994.
25. Nagarathinam, M., Gupta, A., and Davidson, D., "Wind Tunnel Testing of Axisymmetric Air Intake," Technical Report, DRDL, 5120.1003.000, NAL, 1985.
26. Yanta, W.J., Collier, A.S., Spring, C. III, Boyd, W., Christopher, F., and McArthur, J.C., "Experimental Measurements of the Flow in a Scramjet Inlet at Mach 4," *J. of Propulsion*, Vol. 6, No. 6, p. 784-790, 1990.

Table 1. Hydrogen/oxygen chemical kinetics in Arrhenius form, $k = A\,T^N\,e^{-E/RT}$.

Equation	A	N	E/R
$O_2 + H_2 = 2\,OH$	1.700E+13	0	24233
$H_2 + OH = H_2O + H$	2.190E+13	0	2590
$2\,OH = H_2O + O$	6.023E+12	0	550
$H_2 + O = H + OH$	1.800E+10	1	4480
$O_2 + H = O + OH$	1.220E+17	-0.91	8369
$O + H + (M) = OH + (M)$	1.000E+16	0	0
$2\,O + (M) = O_2 + (M)$	2.550E+18	-1	59390
$2\,H + (M) = H_2 + (M)$	5.000E+15	0	0
$H + OH + (M) = H_2O + (M)$	8.400E+21	-2	0

Table 2 Simulation sets with different breakdown criteria in supersonic flow pass a quasi-2-D 25° wedge.

Set	Old Breakdown Criteria	New Breakdown Criteria
Overlapping layers for non-BL	4	4
Overlapping layers for BL	4	25
$Kn^{Thr.}$	Kn_{max} >0.05	Kn_p>0.05
$P_{Ine}^{Thr.}$	0.03	0.03
Final DSMC cells	~ 18,000	~14,000
Sim. particle number	~2,060,000	~1,230,000
Reference Δt (sec)	3.0E-09	
Sampling time steps	10,000	

*Total cell number of computational domain for coupled DSMC-NS method is ~68,000. 10 processors are used throughout the simulation.

Table 3 Total computational time (hours) in supersonic flow pass quasi-2-D 25° wedge.

	Pure NS	Pure DSMC	New coupled method (4 iterations)			Old coupled method (6 iterations)		
			One-shot NS	DSMC	NS	One-shot NS	DSMC	NS
			1.25	3.03	0.63	1.25	9.10	0.57
Total time	1.25	9.33	4.91			10.92		

*The computational time in each iteration for *new* coupled method is about 0.85 hours, while that for *old* coupled method is 1.5 hours.

Table 4 Simulation condition in hypersonic flow over a square cylinder.

Set	New Breakdown Criteria
Overlapping layers	4
$Kn_p^{Thr.}$	0.05
$P_{Ine}^{Thr.}$	0.1
Final DSMC cells	~53,541 (for 20th iteration)
Sim. particle number	~712,000
Reference Δt (sec)	7.36E-08
Sampling time steps	11,000 (Same as in pure DSMC)

*Total cell number of computational domain for coupled DSMC-NS method is 152,500. 10 processors are used.

Table 5 Total computational time (hours) in hypersonic flow pass a square cylinder.

	Pure NS	Pure DSMC	New coupled method (4 iterations)		
			One-shot NS	DSMC	NS
			1.48	2.97	0.55
Total time	1.48	4.17		5.00	

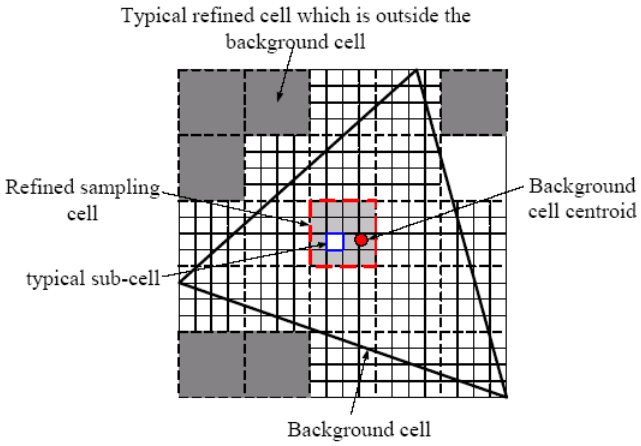

Fig. 1 Typical refined cells (dashed lines) on a triangular background cell (solid lines) along with TAS.

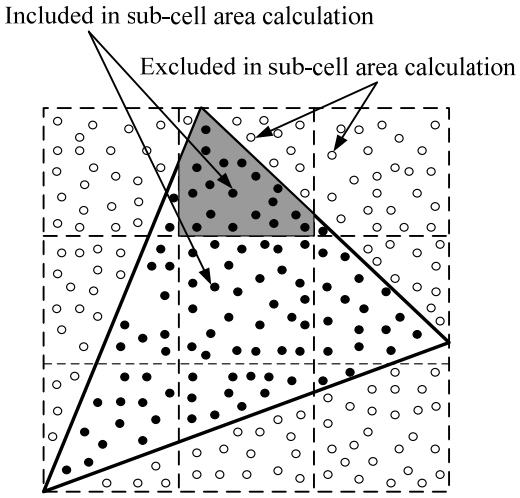

Fig. 2 Sketch of calculating the sub-cell area inside an unstructured background cell using Monte Carlo method.

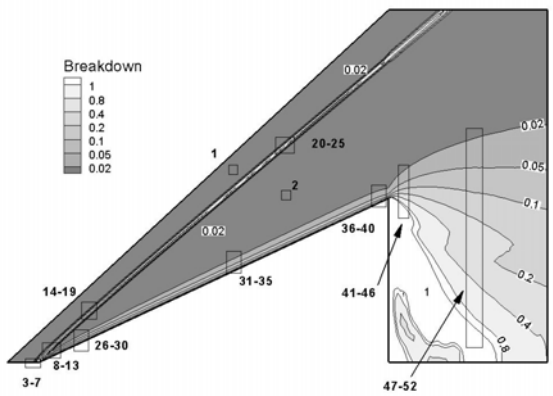

Fig. 3 Sketch of the kinetic velocity sampling locations and distribution of continuum breakdown parameter (based on velocities, density and temperatures) of 2-D 25-degree wedge flow resulting from a pure DSMC simulation.

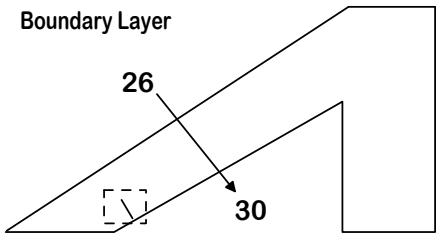

(a)

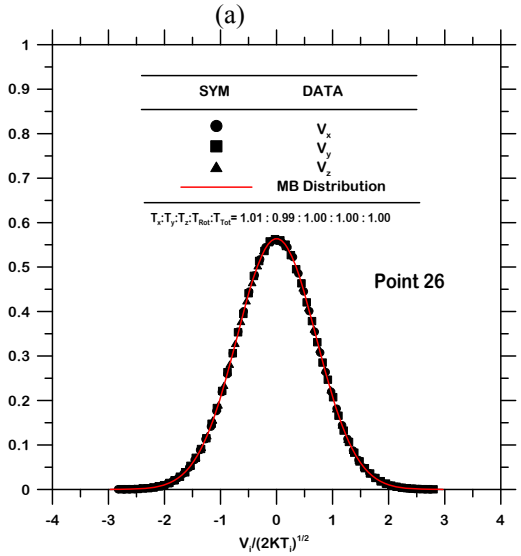

(b)

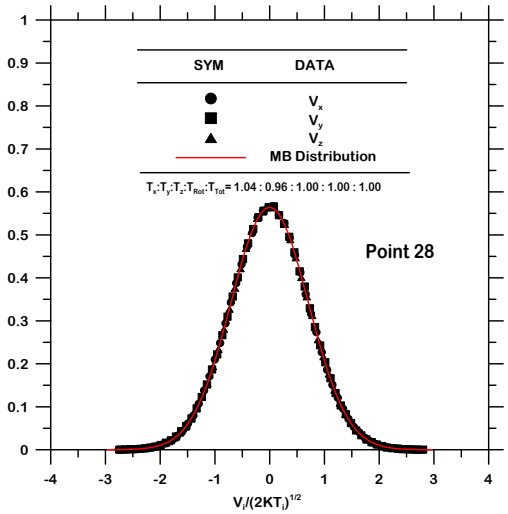

(c)

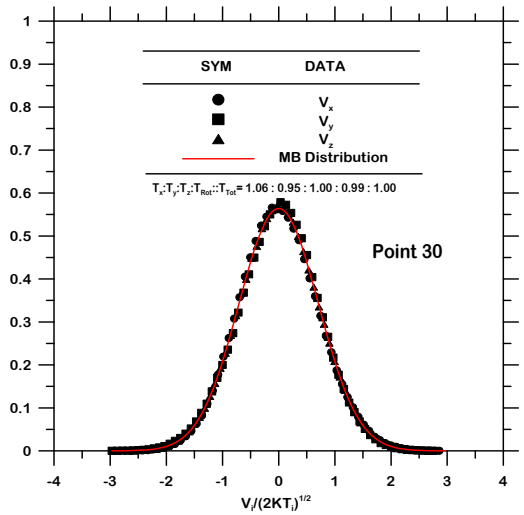

(d)

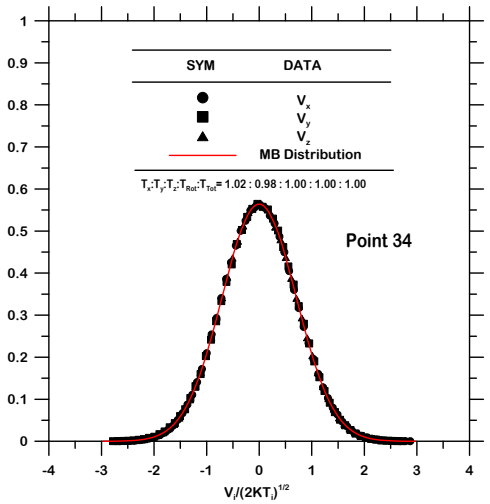

(c)

Fig. 4 (a) Location of sampling points across the boundary layer; Random velocity distributions in each direction at Point (b) 26; (c) 28; (d) 30, along with translational and rotational temperatures.

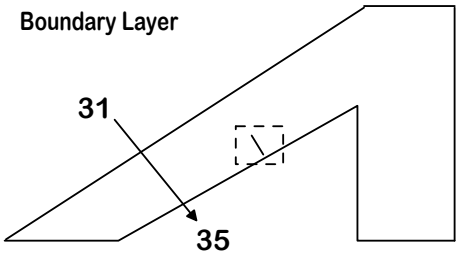

(a)

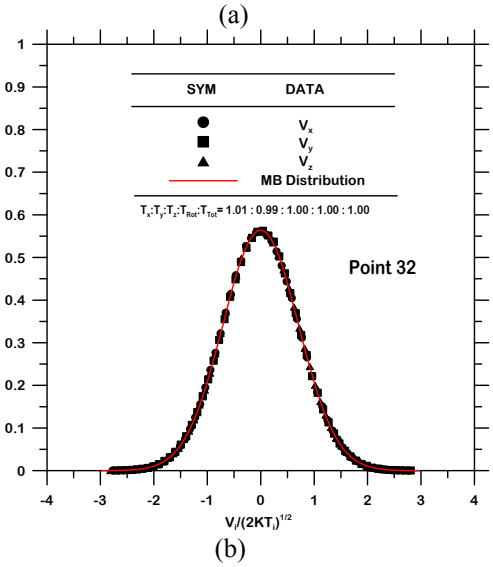

(b)

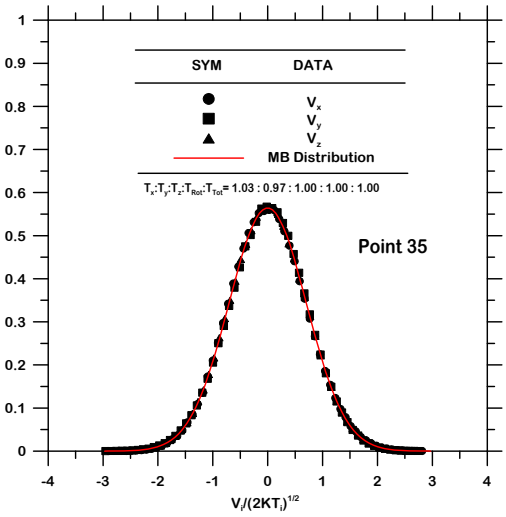

(d)

Fig. 5 (a) Location of sampling points in the boundary layer; Random velocity distributions in each direction at Point (b) 32; (c) 34; (d) 35, along with translational and rotational temperatures.

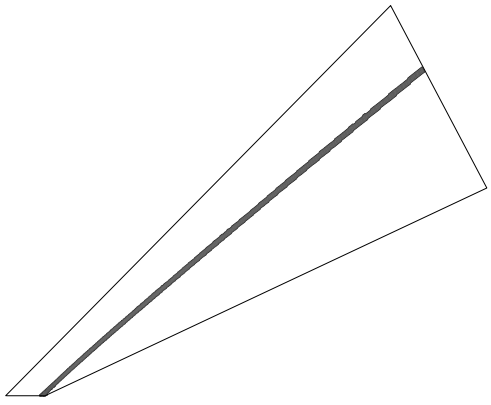

(a)

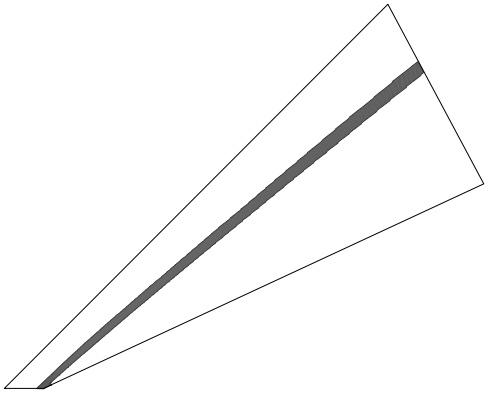

(b)

Fig. 6 Initial continuum breakdown domain with new continuum breakdown criteria (a) Breakdown region (b) DSMC domain including the overlapping regions (Kn_p >0.05).

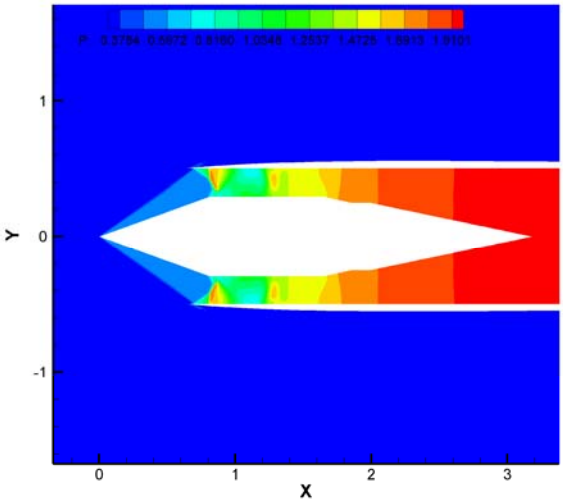

Fig. 7 Predicted ramjet inlet pressure contours.

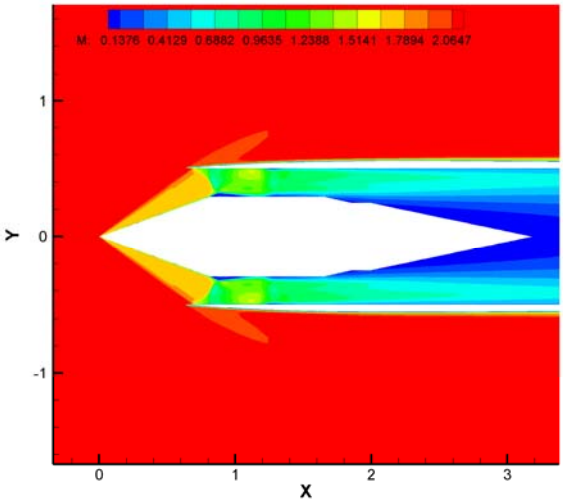

Fig. 8 Predicted ramjet inlet Mach contours.

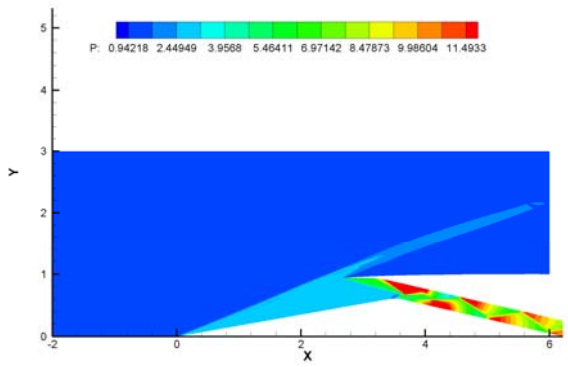

Fig. 9 Scramjet inlet pressure contours.

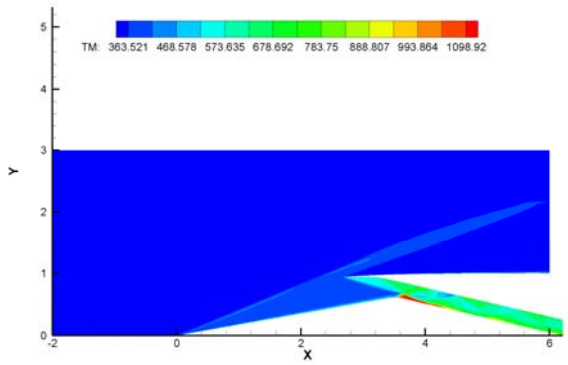

Fig. 10 Scramjet inlet temperature contours.

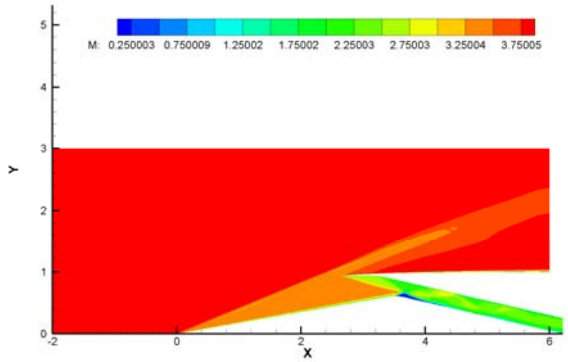

Fig. 11 Predicted inlet Mach number contours.

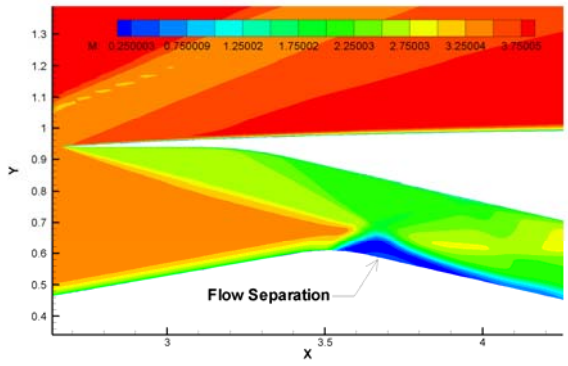

Fig. 12 Flow solution showing inlet separation.

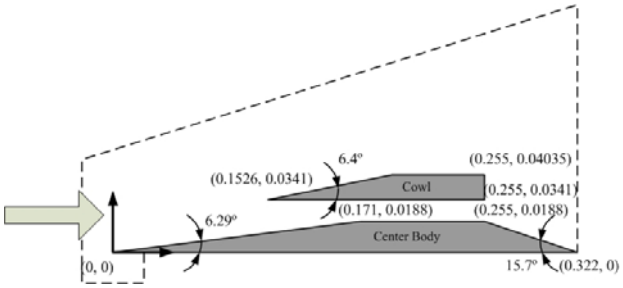

Fig. 13 Sketch of a scramjet flow.

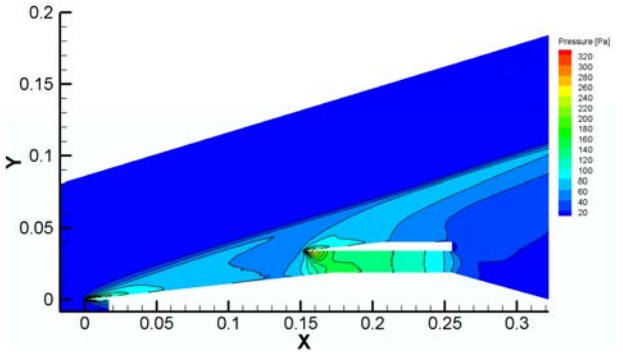

Fig. 14 Pressure contour of a M-15 scramjet flow.

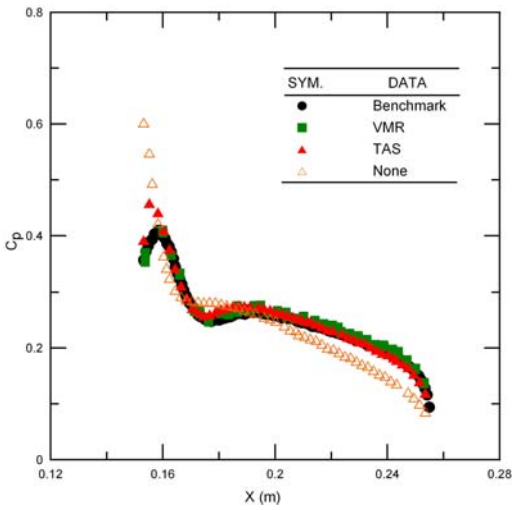

(a)

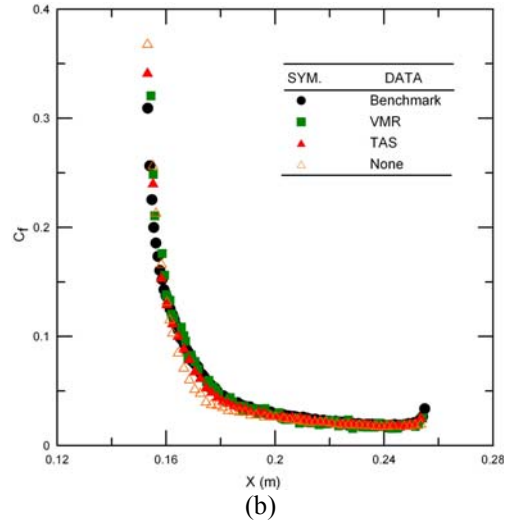

(b)

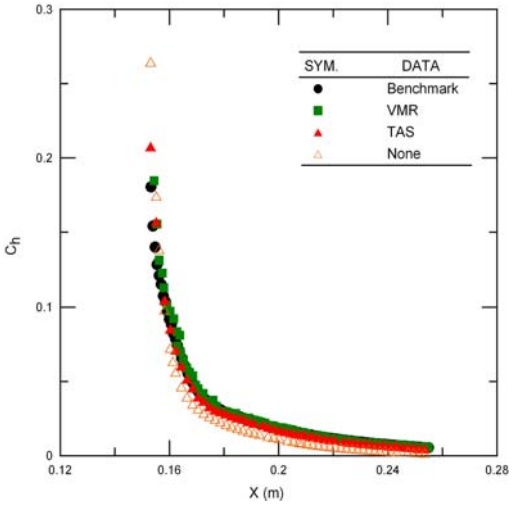

(c)

Fig. 15 Surface property distribution along the top channel wall. (**a**) local pressure coefficient. (**b**) local friction coefficient. (**c**) local heat transfer coefficient.

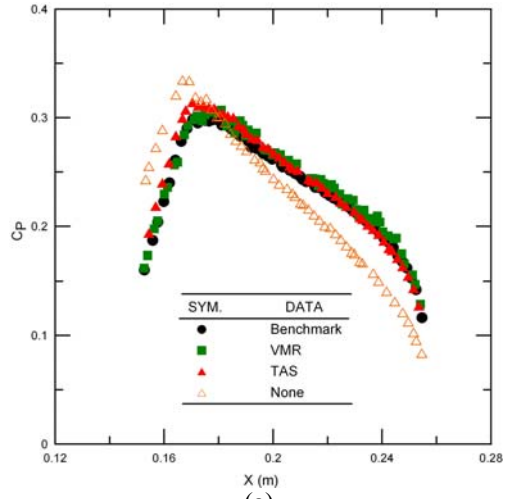

(a)

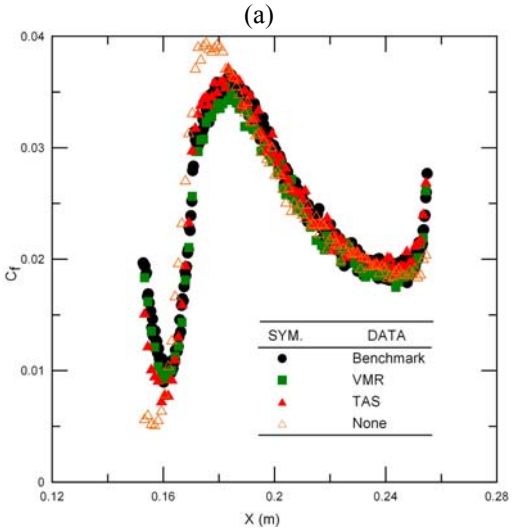

(b)

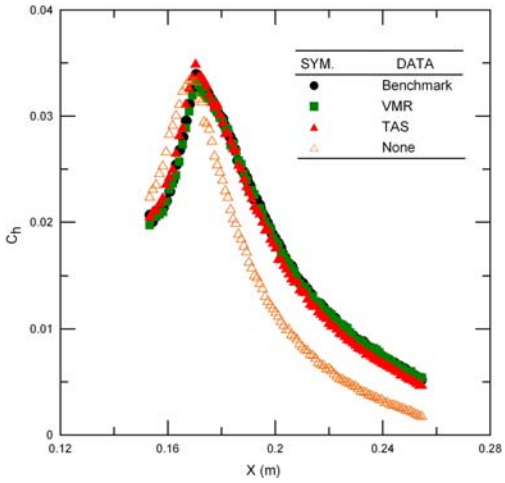

(c)

Fig. 16 Surface property distribution along the bottom channel wall. (**a**) local pressure coefficient. (**b**) local friction coefficient. (**c**) local heat transfer coefficient.

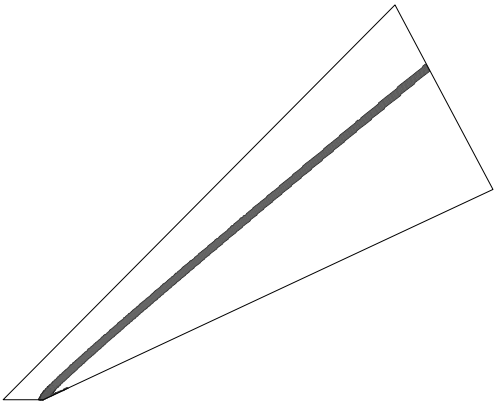

(a)

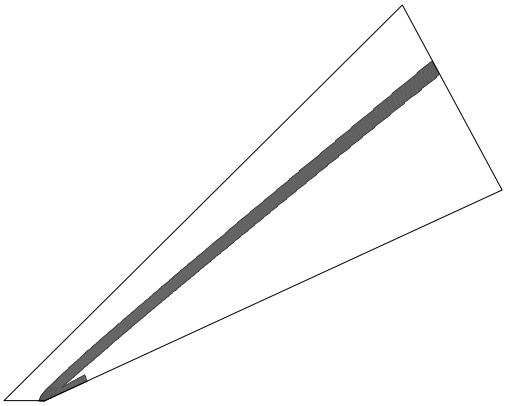

(b)

Fig. 17 Breakdown domain distribution at 20th hybrid iteration with new continuum breakdown criteria (a) Breakdown region (b) DSMC domain including the overlapping regions.

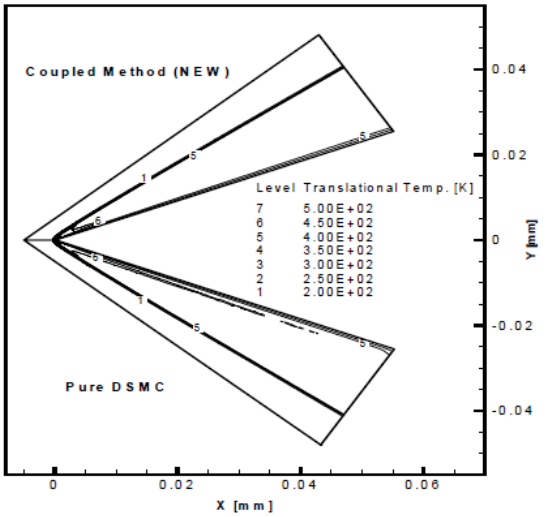

(a)

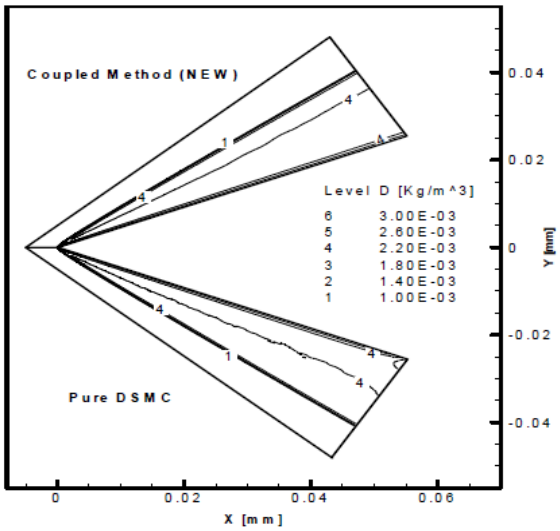

Fig. 18 (a) Density and (b) Translation temperature comparison between the DSMC method and the present coupled DSMC-NS method in quasi-2-D 25° wedge flow.

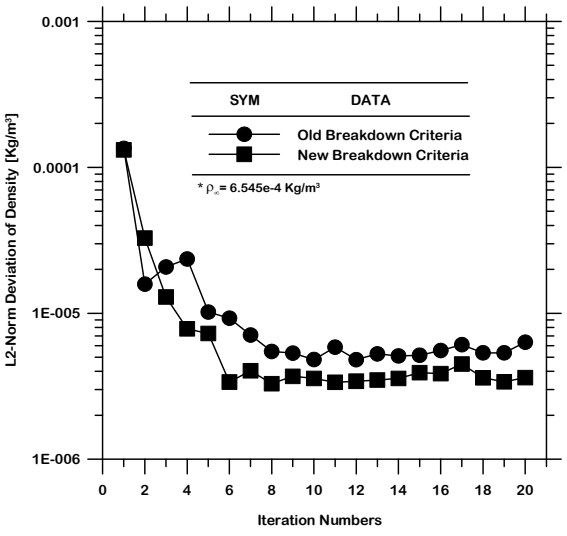

(a)

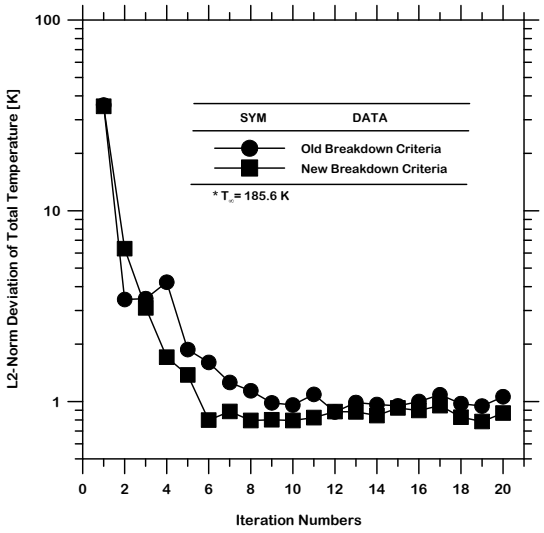

(b)

Fig. 19 Convergence history of L2-norm deviation of (a) density and (b) overall temperature between different continuum breakdown criteria in quasi-2-D 25° wedge flow.

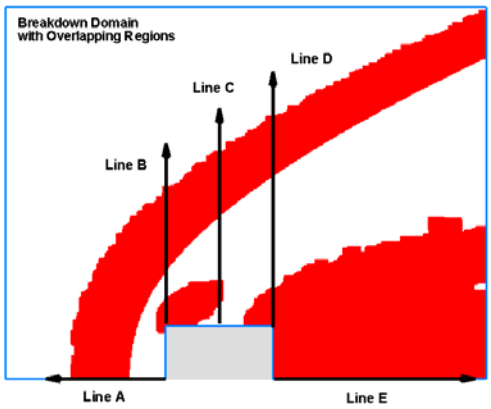

Fig. 20 Final breakdown regions and locations of Line A, B, C, D and E (for 20th iterations). Breakdown regions are shown in red color.

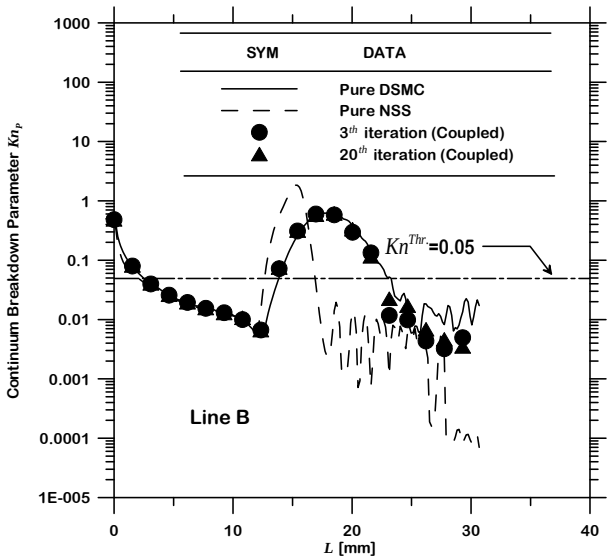

Fig. 21 Profiles of Continuum breakdown parameter along Line B.

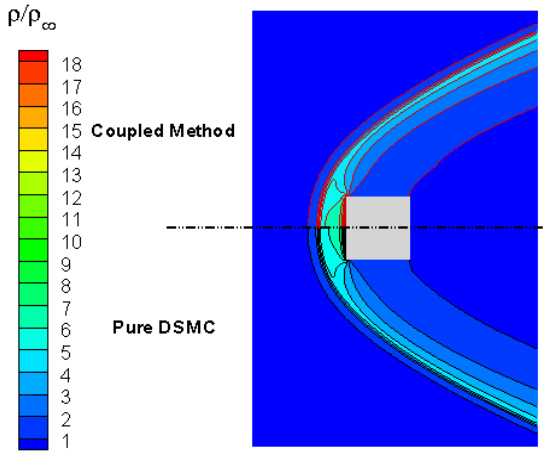

(a)

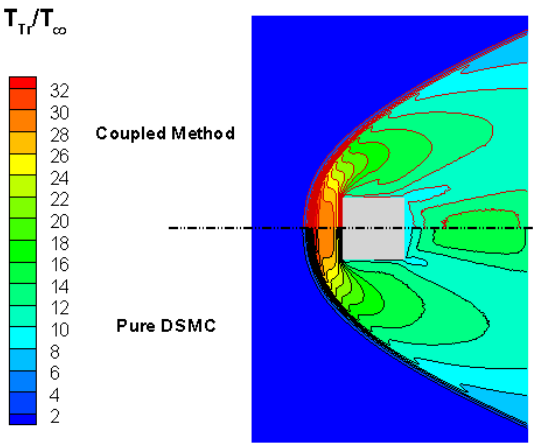

(b)

Fig.22 (a) Density and (b) translational temperature comparison between the DSMC method and the present coupled DSMC-NS method in

hypersonic flow pass a square cylinder (for 20 iterations).

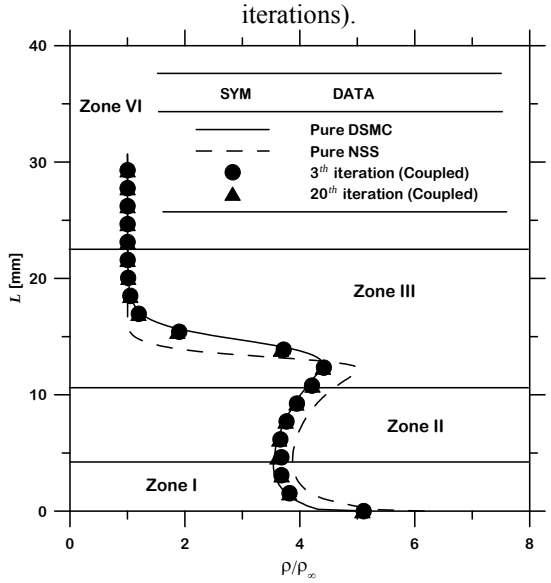

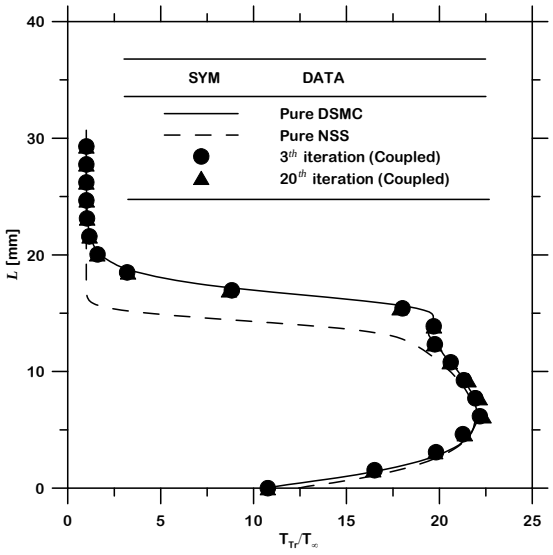

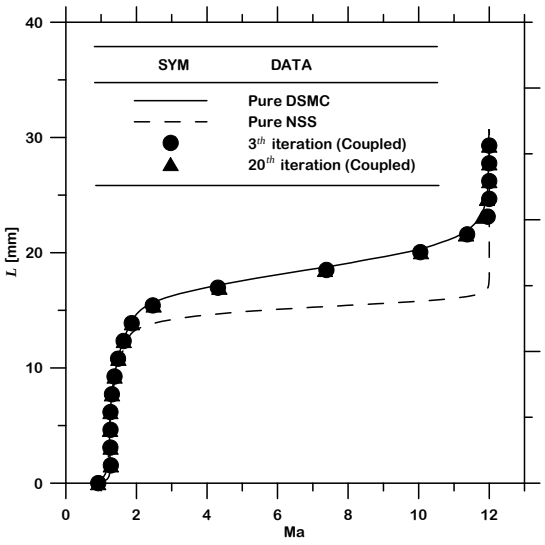

Fig. 23 Profile of (a) density, (b) translational temperature and (c) Mach number along Line B.